NANO LETTERS

2007
Vol. 7, No. 2
421−425

Structural and Morphological Characterization of Cerium Oxide Nanocrystals Prepared by Hydrothermal Synthesis

Kenji Kaneko,*,† Koji Inoke,‡ Bert Freitag,§ Ana B. Hungria,|| Paul A. Midgley,|| Thomas W. Hansen,⊥ Jing Zhang,# Satoshi Ohara,# and Tadafumi Adschiri#

Department of Materials Science & Engineering, Kyushu University, 744, Motooka, Nishi, Fukuoka, 819-0395, Japan, FEI Company Japan Ltd., 13-34, Kohnan 2, Minato, Tokyo, 108-0075, Japan, FEI Company, Achtseweg Noord 5, P.O. Box 218, 56000 MD Eindhoven, The Netherlands, Department of Materials Science and Metallurgy, University of Cambridge, Pembroke Street, Cambridge, CB2 3QZ, U.K., Department of Inorganic Chemistry, Fritz-Haber-Institute (MPG), Faradayweg 4-6, D-14195 Berlin, Germany, and Insistute of Multidisciplinary Research for Advanced Materials, Tohoku University, 2-1-1, Katahira, Aoba-ku, Sendai 980-8577, Japan

Received November 15, 2006; Revised Manuscript Received January 5, 2007

ABSTRACT

Colloidal cerium oxide (CeO_2) nanocrystals prepared by hydrothermal synthesis were characterized by high-resolution transmission electron microscopy (HRTEM) and three-dimensional electron tomography (3D-ET). HRTEM images of individual CeO_2 nanocrystals were then simulated by Blochwave and multislice simulations to determine the atomic arrangement and terminating atoms. The edge length distributions were between 5.0 and 8.0 nm with an average edge length of 6.7 nm. The HRTEM images showed that the CeO_2 particles were slightly truncated revealing {220} facets. 3D-ET revealed that the CeO_2 nanocrystals exposed predominantly {200} cubic facets. The nanocrystals were truncated at the corners exposing {111} octahedral facets and at the edges {220} dodecahedral facets. Furthermore, 3D-ET revealed the presence of some tetragonal-shaped CeO_2 nanocrystals.

The solid oxide fuel cell (SOFC) has attracted increasing attention in recent years, because of its high-energy conversion efficiency and environmental friendliness, and is considered as a new clean power source for this century.[1−4] For this purpose, there has been increasing interest in the synthesis of cerium oxide (CeO_2), which can be used as an oxygen conductor in SOFCs, for various electrocatalytic applications and for direct production of hydrogen from methanol.[5] From the viewpoint of increasing catalytic activities, it is necessary to synthesize CeO_2 nanocrystals with a large surface area and with highly active facets, namely, {200} facets, which would offer the largest possible number of active sites for catalytic reactions.[6−8] In fact, CeO_2 {200} facets are energetically the most unstable among the low-index CeO_2 {111}, {220}, and {200} facets.[6]

Several researchers have already carried out various methods to prepare CeO_2 nanocrystals. Among these methods are precipitation,[9] urea decomposition,[10] combustion,[11] thermal decomposition,[12] spray pyrolysis,[13] microemulsion,[14] and electrochemical synthesis.[15] Recently, preparation of nanocrystal CeO_2 by hydrothermal synthesis was developed.[16]

In this paper, structural and morphological characterizations of CeO_2 nanocrystals prepared by hydrothermal synthesis were carried out using high-resolution transmission electron microscopy (HRTEM) and three-dimensional electron tomography (3D-ET). Furthermore, image simulations were carried out to examine the surface termination of the CeO_2 nanocrystals.

Cerium oxide was prepared by mixing 100 mL of 0.1 M $Ce(NO_3)_3$ solution with 100 mL of 0.3 M NaOH and stirring for about 6 h. The precursor was centrifuged and washed several times with distilled water in a vessel. Decanoic acid (0.05−1.00 g) was added to modify the surfaces and induce anisotropic growth of the nanocrystals. The hydrothermal synthesis was carried out at 400 °C for 10 min in the vessel

† Kyushu University.
‡ FEI Company Japan Ltd.
§ FEI Company.
|| University of Cambridge.
⊥ Fritz-Haber-Institute (MPG).
Tohoku University.

10.1021/nl062677b CCC: $37.00
Published on Web 01/13/2007

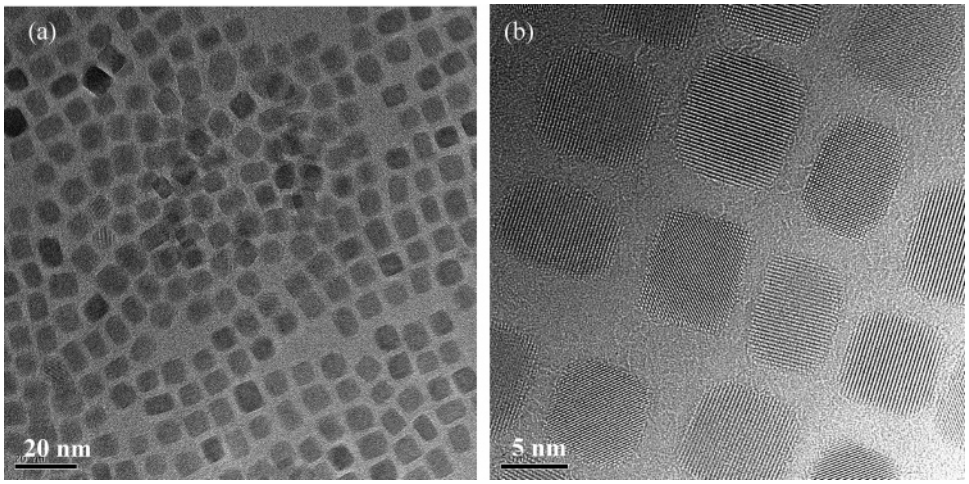

Figure 1. Characteristic TEM images of CeO_2 nanocrystals at different magnifications.

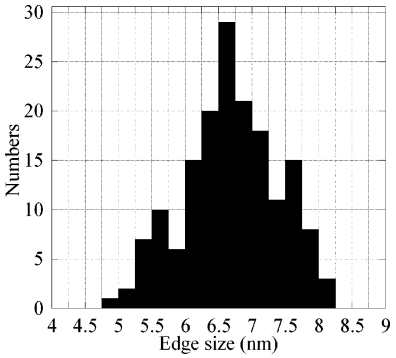

Figure 2. The edge length distribution of CeO_2 nanocrystals.

and terminated by submerging into a water bath at room temperature. The organic-ligand-modified nanocrystals were extracted from the product mixture with 3 mL of hexane. The final products were precipitated from the resulting hexane phase by the addition of 10 mL of ethanol as an antisolvent reagent and then separated by centrifugation. The solution with nanocrystals was then dropped onto amorphous carbon specimen grids for preparing a TEM specimen.

Structural and morphological characterizations of the CeO_2 nanocrystals were carried out in a spherical aberration (Cs) corrected transmission electron microscope operated at 300 kV (TITAN 80-300, FEI, The Netherlands). 3D-ET observations were conducted using a scanning TEM with a high-angle annular dark-field (STEM-HAADF) detector operated at 200 kV (TECNAI-F20, FEI, The Netherlands) with a specially designed high-tilt holder (E. A. Fischione Instruments Inc., U.S.A.). In the case of 3D-ET, many TEM parameters were controlled during the acquisition of the tilt series of projections: defocus, image shift, specimen tilt, and the condenser lens astigmatism. Data collection for 3D-ET was carried out by tilting the specimen about a single axis with respect to the electron beam. A series of projections was acquired with the specimen tilt varying from −70° to 74°, with a STEM-HAADF image recorded every 2° giving a total of 73 images. A HAADF detector collects electrons that undergo high-angle scattering, and the signal is approximately proportional to Z^2, where Z is the atomic number. 3D-ET with Z-contrast imaging is useful in the study of (poly)crystalline materials because of the reduction of coherent diffraction contrast, which is unwanted for tomographic reconstructions.[17−19]

Once the acquisition of the tilt series was completed, images were spatially aligned by a cross-correlation algorithm

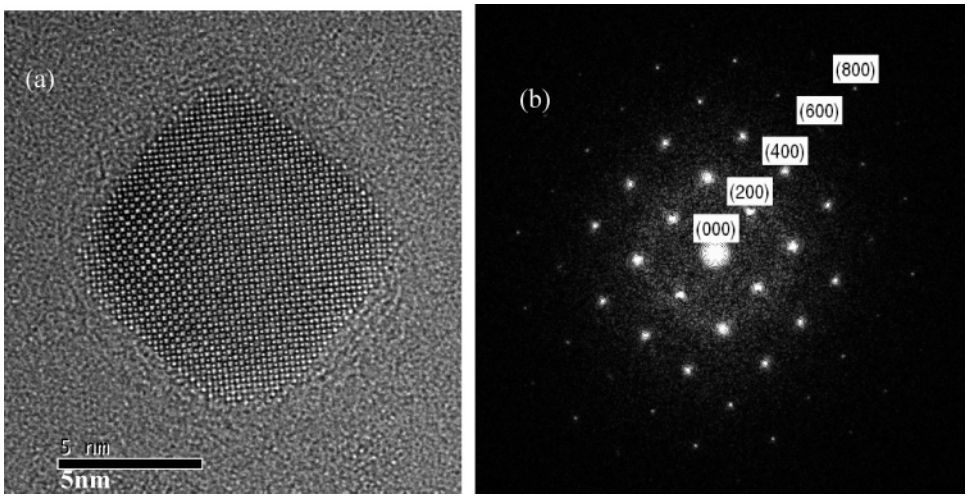

Figure 3. (a) A HRTEM image of an individual CeO_2 nanocrystal viewed in the [001] direction and (b) its Fourier transform.

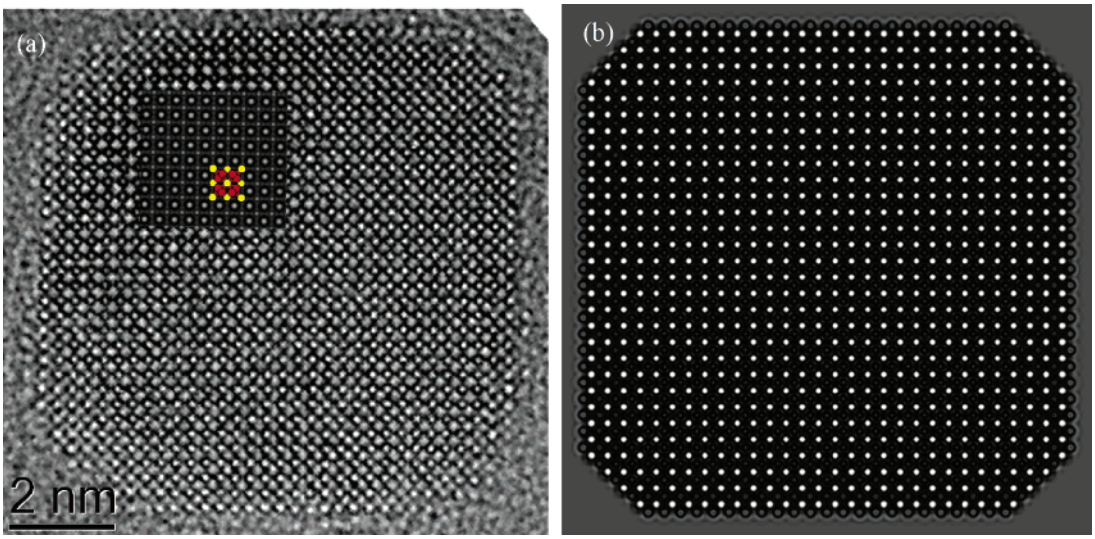

Figure 4. (a) HRTEM image of a CeO_2 nanocrystal viewed in the [001] zone axis. Truncation of each edge is clearly seen from HRTEM image. A simulated image is superimposed onto the experimental image, Yellow = Ce, red = O, respectively. (b) A multislice simulation of a CeO_2 particle of a particle of similar size and truncation.

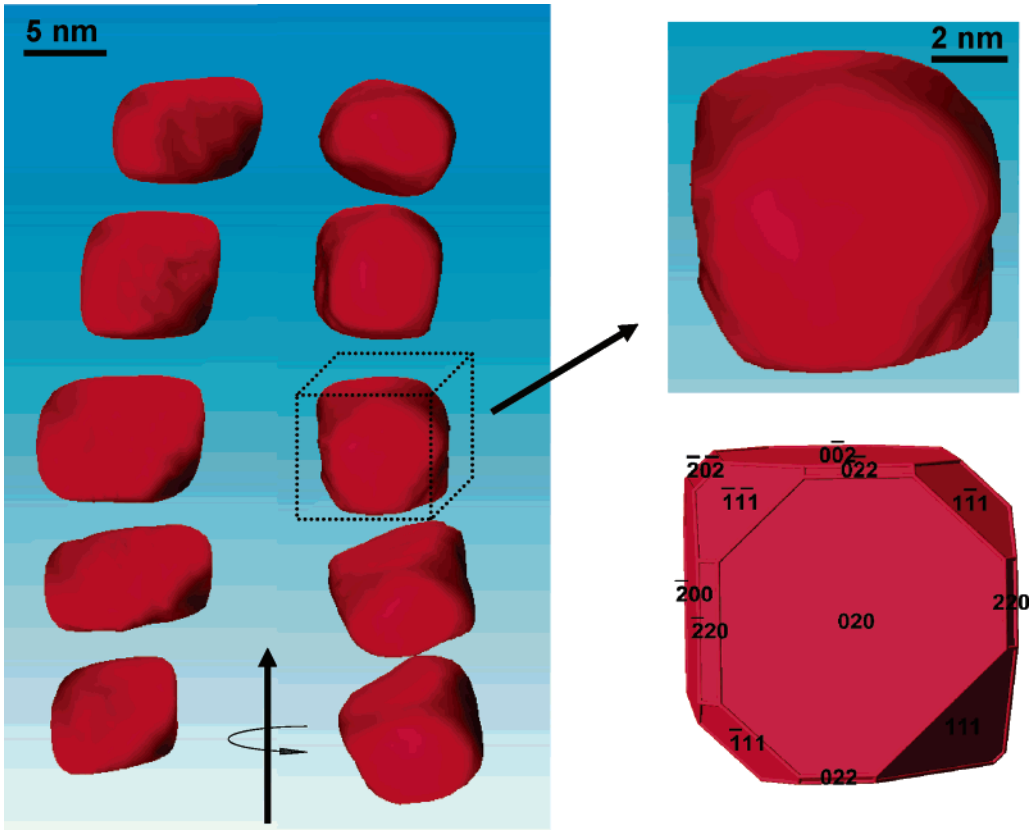

Figure 5. 3D volume rendered images indicating the presence of {111} at each corner and {220} at each edge.

using Inspect3D software (FEI, The Netherlands), and 3D reconstructions were achieved using a simultaneous iterative reconstruction algorithm (SIRT) of consecutive 2D slices. Visualization was performed using AMIRA 4.0.

HRTEM image simulations were carried out using the JEMS program. The input structure was created from the data of Yashima and Kobayashi.[20] For both Blochwave and multislice simulations, the aspect ratio of nanoparticles, perpendicular to the electron beam, was assumed as 1. Thus the thickness of the simulated structure was the same as the width of the structure. All microscope parameters for the simulations were the same as those used for the experimental images.

Figure 1 shows characteristic TEM images of the CeO_2 nanocrystals prepared by hydrothermal synthesis on amorphous carbon grid. CeO_2 is a fluorite-structured material with the calculated lattice constant 0.543 nm. The crystallites are oriented predominantly along the [001] zone axis exposing

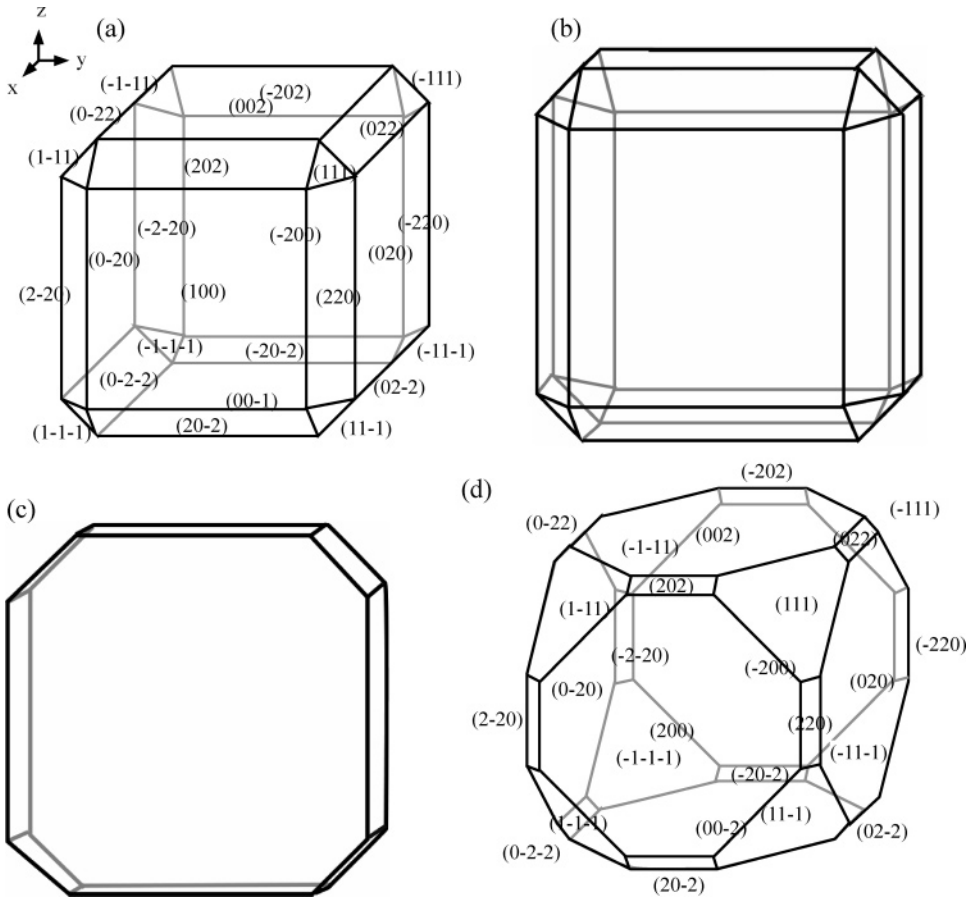

Figure 6. Proposed morphologies of the CeO_2 nanocrystals: (a−c) from HRTEMand (d) from a combination of HRTEM and 3D-ET.

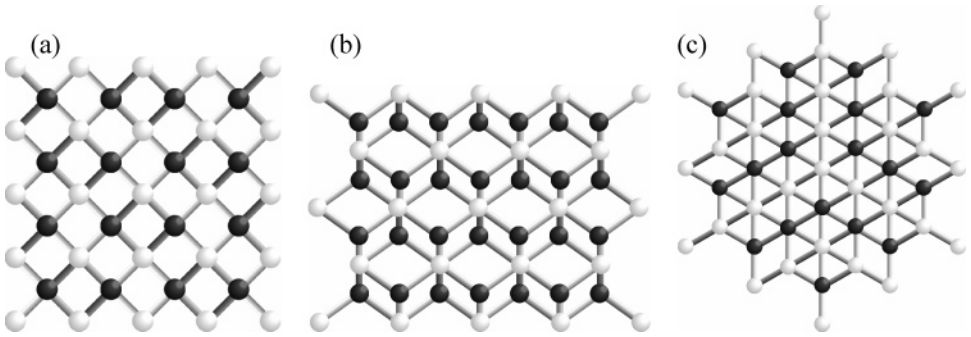

Figure 7. The ideal CeO_2 structure seen from (a) [001], (b) [011], and (c) [111] directions. White circles and dark gray circles are representing Ce and O atoms, respectively.

lattice fringes corresponding to the {200} facets. The apparent aspect ratio of most of the particles, the plane perpendicular to the electron beam, is close to 1, but some nanocrystals have apparent aspect ratios as high as 1.4, because the CeO_2 nanocrystals would have been tilted toward [110] direction and because they are possibly tetragonal, as can be seen from Figure 1.

The TEM images revealed that the edge length of the CeO_2 nanocrystals ranges between 5 and 8 nm with average edge length about 6.7 nm, as shown in Figure 2.

No obvious defects or dislocations were observed from the HRTEM images of individual CeO_2 nanocrystals, Figure 3a. Furthermore the TEM images reveal that surfaces of the CeO_2 nanocrystals are even and without any steps on the {001} surfaces, and the truncations at the {220} facets are observed. Therefore, the synthesized CeO_2 nanocrystals are nonporous with well-defined crystalline structures. In order to characterize these CeO_2 nanocrystals, fast Fourier transforms of the CeO_2 nanocrystals were obtained from the particles as shown in Figure 3b.

For the image simulations the Cs of the microscope was set to -10 μm. The simulation shows that a defocus value of -7 nm and a thickness of 9 nm, superimposed onto the image, appear to be in good agreement with the experimental data. It should be noted that the CeO_2 (200) surface is terminated with Ce atoms.

Truncations of corners were not clear from two-dimensional images. However, the result of 3D-ET volume

rendered images confirmed the presence of {111} at corners, observed from different orientations, as shown in Figure 5 and Supporting Information.

Although, the morphology of the CeO_2 nanocrystals was predicted from the HRTEM image as that shown in parts a−c of Figure 6 with the presences of {220} facets at edges, the shape of {111} facets seen in parts a and b of Figure 6 was found to be inverse from that in Figure 5 and Figure 6d. The area of {220} can be narrower so that the facet of {111} could be closer to the triangular shape, as can be seen in Figure 5.

CeO_2 is the binary solid oxide of cerium. It crystallizes in the fluorite structure with each Ce^{4+} cation surrounded by eight equivalent nearest O^{2-} anions forming the corners of a cube, with each O^{2-} anion surrounded by a tetrahedron of four cerium ions, as shown in Figure 7, seen from different orientations. In the case of CeO_2 nanocrystals, the organic ligands might have increased the configurational entropy and caused the truncations of {220} and {111} facets of the cubic crystallites. The CeO_2 nanocrystals were presumed to nucleate and grow cubic and tetragonal structures predominantly during the hydrothermal synthesis with truncations of {220} and {111} facets.

In summary, we characterized the CeO_2 nanocrystals prepared by hydrothermal synthesis with HRTEM, image simulation, and 3D-ET. The edge length distributions were found to range between 5.0 and 8.0 nm with an average edge length of 6.7 nm. The apparent aspect ratios of the edges varied from 1.0 to 1.4 due to the presence of cubic structures tilted from the [100] to [110] direction and that of the tetragonal-shaped CeO_2 nanocrystals. In addition, image simulation of the HRTEM image showed that the CeO_2 nanocrystals were slightly truncated at edges revealing {220} facets. 3D-ET revealed that the CeO_2 nanocrystals exposed predominantly {200} cubic facets with truncations of the corners exposing {111} facets and at the edges showing {220} facets. Furthermore, 3D-ET revealed the presence of some tetragonal-shaped CeO_2 nanocrystals as observed from the TEM observations.

Nanoscale characterization plays a vital role in both the design and property of materials used in nanotechnology. So far, large numbers of papers have been published concerning nanoscale materials based on TEM images which display 2D projected images, which is not exactly reflecting the true 3D morphologies of the materials, and authors had to correlate those results with 3D physical properties of nanoscale materials. We would like to emphasize that both 2D information and 3D information are vital to characterize three-dimensional nanoscale materials.

Acknowledgment. This work was supported in part by "Grant-in-Aid for the 21st Century COE Program (Functional Innovation of Molecular Informatics)" and "Grant-in-Aid for the 21st Century COE Program (Giant Molecules and Complex Systems)" of the Ministry of Education, Culture, Sports, Science and Technology of Japan. P.A.M. thanks the Isaac Newton Trust for funding and the Royal Academy of Engineering and the Leverhulme Trust for the award of Senior Research Fellowships. A.B.H. thanks the European Community for a Marie Curie Research Fellowship.

Supporting Information Available: A video showing a 3D view of the nanocrystal structure. This material is available free of charge via the Internet at http://pubs.acs.org.

References

(1) Inaba, H.; Tagawa, H. *Solid State Ionics* **1996**, *83*, 1−16.
(2) Arai, H.; Kunisaki, T.; Shimizu, Y.; Seiyama, T. *Solid State Ionics* **1986**, *20*, 241−248.
(3) Yahiro, H.; Eguchi, K.; Arai, H. *Solid State Ionics* **1989**, *36*, 71−75.
(4) Mogensen, M.; M. Sammes, N.*; Tompett, G. A. Solid State Ionics* **2000**, *129*, 63−94.
(5) Mo, L.; Zheng, X.; Yeh, C-T. *Chem. Commun.* **2004**, 1426−1427.
(6) Sayle, T. X. T.; Parker, S. C.; Catlow, C. R. A. *Surf. Sci.* **1994**, *316*, 329−336.
(7) Yu, J. C.; Zhang, L.; Lin, J. *J. Colloid Interface Sci.* **2003**, *260*, 240−243.
(8) Wang, Z. L.; Feng, X. D. *J. Phys. Chem. B* **2003**, *107*, 13563−13566.
(9) Fierro, J. L. G.; Mendioroz, S.; Olivan, A. M. *J. Colloid Interface Sci.* **1984**, *100*, 303−310.
(10) Matijevic, E.; Hsu, W. P. *J. Colloid Interface Sci.* **1987**, *118*, 506−523.
(11) Varma, H. K.; Mukundan, P.; Warrier, K. G. K.; Damodaran, A. D. *J. Mater. Sci. Lett.* **1990**, *9*, 377−379.
(12) Guillou, N.; Auffredic, J. P.; Louër, D. *J. Solid State Chem.* **1995**, *115*, 295−298.
(13) Okuyama, K.; Lenggoro, I. W. *Chem. Eng. Sci.* **2003**, *58*, 537−547.
(14) Masui, T.; Fujiwara, K.; Machida, K.; Adachi, G.; Sakata, T.; Mori, H. *Chem. Mater.* **1997**, *9*, 2197−2204.
(15) Zhou, Y.; Phillips, R. J.; Switzer, J. A. *J. Am. Ceram. Soc.* **1995**, *78*, 981−985.
(16) Zhang, J.; Ohara, S.; Umetsu, M.; Naka, T.; Hatakeyama, Y.; Adschiri, T. *Adv. Mater.*, in press.
(17) Midgley, P. A.; Weyland, M. *Ultramicroscopy* **2003**, *96*, 413−431.
(18) Kübel, C.; Voigt, A.; Schoenmakers, R.; Otten, M.; Su, D.; Lee, T-C.; Carlsson, A.; Bradley, J. *Microsc. Microanal.* **2005**, *11*, 378−400.
(19) Inoke, K.; Kaneko, K.; Weyland, M.; Midgley, P. A.; Higashida, K.; Horita, Z. *Acta Mater.* **2006**, *54*, 2957−2963.
(20) Yashima, M.; Kobayashi, S. *Appl. Phys. Lett.* **2004**, *84*, 526−528.

NL062677B